

## **Heat Transfer on Peristaltically Induced Walter's B Fluid Flow**

Obaid Ullah Mehmood, Norzieha Mustapha, and Sharidan Shafie

Department of Mathematics, Faculty of Science, Universiti Teknologi Malaysia, Johor, Malaysia

This paper look at the effects of heat transfer on peristaltic flow of Walter's B fluid in an asymmetric channel. The regular perturbation method is used to solve the governing equations by taking the wave number as the small parameter. Expressions for stream function, temperature distribution, and heat transfer coefficient are presented in explicit form. Solutions are analyzed graphically for different values of arising parameters. It has been found that these parameters affect considerably the considered flow characteristics. Results show that with an increase in the Eckert and Prandtl numbers, the temperature and heat transfer coefficient increase. Further, the absolute value of the heat transfer coefficient increases with an increasing viscoelastic parameter. Comparison with published results for viscous fluid is also presented. © 2012 Wiley Periodicals, Inc. *Heat Trans Asian Res*, 41(8): 690–699, 2012; Published online 1 November 2012 in Wiley Online Library (wileyonlinelibrary.com/journal/htj). DOI 10.1002/htj.21021

**Key words:** heat transfer, peristaltic flow, Walter's B fluid, heat transfer coefficient

### **1. Introduction**

Peristalsis is an inherited mode of fluid transport in living tracts induced by the wavy motion of the boundaries. This wavy motion is sinusoidal in nature [1] and responsible for mixing and transportation of the contents within the tracts. Peristalsis is involved in the motion of food in the gastrointestinal tract, motion of secretions in glandular ducts, transport of urine in the cervical canal, and others. In industrial applications, artificial hearts and ortho-pumps, heart lung machines, transport of toxic material, and waste inside the sanitary ducts involve peristalsis. The above-mentioned situations usually involve a fluid having non-Newtonian behavior with some elastic properties because most of them are a suspension of particles in Newtonian fluid with fading memory. Walter's B fluid model with limiting viscosity at low shear rates and short memory coefficient [2] is the best model for the above mentioned situations [3–5].

Heat transfer analysis of the flow of physiological fluids induced by the peristaltic waves is imperative in many realistic situations like oxygenation, hemodialysis, heat conduction, metabolic processes, internal heat generation, and others. It is also useful in the treatment of diseased tissues in

---

Contract grant sponsor: Ministry of Higher Education (MOHE) and Research Management Centre—UTM for the financial support through vote numbers 03J54, 78528, and 4F109.

cancer. Recent investigations on the peristaltic flows with heat transfer include numerous studies [6–12]. Peristaltic flow of Walters’ B fluid in an inclined tube is considered by Nadeem and Akbar [13]. Moreover, Nadeem et al. [14] studied the peristaltic flow of Walters’ B fluid in an endoscope. Much attention has been paid to heat transfer analysis of viscous and non-Newtonian fluids. However, no one has investigated the heat transfer analysis on the peristaltic flow of viscoelastic fluid in an asymmetric channel, which is of great interest in many physiological flows. Motivated by these facts, in the present problem, the heat transfer analysis of a peristaltic flow of Walter’s B fluid in an asymmetric channel is studied.

## 2. Formulation of the Problem

A two-dimensional flow of an incompressible viscoelastic Walter’s B fluid in an asymmetric channel is considered. The fluid motion is governed by the propagation of sinusoidal waves with different amplitudes and phases moving along the walls of the channel. The upper and lower walls are at distance  $d_1$  and  $d_2$  from the centerline ( $Y = 0$ ) of the channel and maintained at temperature  $T_0$  and  $T_1$ , respectively.

The continuity, momentum, and energy equations are given by

$$\frac{\partial \bar{U}}{\partial \bar{X}} + \frac{\partial \bar{V}}{\partial \bar{Y}} = 0 \quad (1)$$

$$\rho \left( \frac{\partial}{\partial \bar{t}} + \bar{U} \frac{\partial}{\partial \bar{X}} + \bar{V} \frac{\partial}{\partial \bar{Y}} \right) \bar{U} = - \frac{\partial \bar{P}(\bar{X}, \bar{Y}, \bar{t})}{\partial \bar{X}} + \frac{\partial \bar{S}_{\bar{X}\bar{X}}}{\partial \bar{X}} + \frac{\partial \bar{S}_{\bar{X}\bar{Y}}}{\partial \bar{Y}} \quad (2)$$

$$\rho \left( \frac{\partial}{\partial \bar{t}} + \bar{U} \frac{\partial}{\partial \bar{X}} + \bar{V} \frac{\partial}{\partial \bar{Y}} \right) \bar{V} = - \frac{\partial \bar{P}(\bar{X}, \bar{Y}, \bar{t})}{\partial \bar{Y}} + \frac{\partial \bar{S}_{\bar{X}\bar{Y}}}{\partial \bar{X}} + \frac{\partial \bar{S}_{\bar{Y}\bar{Y}}}{\partial \bar{Y}} \quad (3)$$

$$\rho \xi \left( \frac{\partial}{\partial \bar{t}} + \bar{U} \frac{\partial}{\partial \bar{X}} + \bar{V} \frac{\partial}{\partial \bar{Y}} \right) T = k \left( \frac{\partial^2 T}{\partial \bar{X}^2} + \frac{\partial^2 T}{\partial \bar{Y}^2} \right) + \bar{U}_{\bar{X}} \bar{S}_{\bar{X}\bar{X}} + (\bar{U}_{\bar{Y}} + \bar{V}_{\bar{X}}) \bar{S}_{\bar{X}\bar{Y}} + \bar{V}_{\bar{Y}} \bar{S}_{\bar{Y}\bar{Y}} \quad (4)$$

where

$$\bar{S}_{\bar{X}\bar{X}} = \eta_0 (4\bar{U}_{\bar{X}}) - k_0 (4\bar{U}_{\bar{X}\bar{t}} + 4\bar{U}\bar{U}_{\bar{X}\bar{X}} + 4\bar{V}\bar{U}_{\bar{X}\bar{Y}} - 8\bar{U}_{\bar{X}}^2 - 4\bar{V}_{\bar{X}}\bar{U}_{\bar{Y}} - 4\bar{V}_{\bar{X}}^2). \quad (5)$$

$$\begin{aligned} \bar{S}_{\bar{X}\bar{Y}} &= \eta_0 (2\bar{U}_{\bar{Y}} + 2\bar{V}_{\bar{X}}) - k_0 (2\bar{U}_{\bar{Y}\bar{t}} + 2\bar{V}_{\bar{X}\bar{t}} + 2\bar{U}\bar{U}_{\bar{X}\bar{Y}} + 2\bar{U}\bar{V}_{\bar{X}\bar{X}} + 2\bar{V}\bar{U}_{\bar{Y}\bar{Y}} + 2\bar{V}\bar{V}_{\bar{X}\bar{Y}} - 6\bar{U}_{\bar{X}}\bar{U}_{\bar{Y}} \\ &\quad - 2\bar{U}_{\bar{Y}}\bar{V}_{\bar{Y}} - 2\bar{U}_{\bar{X}}\bar{V}_{\bar{X}} - 6\bar{V}_{\bar{X}}\bar{V}_{\bar{Y}}). \end{aligned} \quad (6)$$

$$\bar{S}_{\bar{Y}\bar{Y}} = \eta_0 (4\bar{V}_{\bar{Y}}) - k_0 (4\bar{V}_{\bar{Y}\bar{t}} + 4\bar{U}\bar{V}_{\bar{X}\bar{Y}} + 4\bar{V}\bar{V}_{\bar{Y}\bar{Y}} - 4\bar{U}_{\bar{Y}}^2 - 4\bar{V}_{\bar{X}}\bar{U}_{\bar{Y}} - 8\bar{V}_{\bar{Y}}^2) \quad (7)$$

with boundary conditions, and the geometries of the walls  $\bar{H}_1$  and  $\bar{H}_2$  are defined by

$$\bar{U} = 0, \quad T = T_0, \quad \text{at } \bar{Y} = \bar{H}_1 \quad (8)$$

$$\bar{U} = 0, \quad T = T_1, \quad \text{at } \bar{Y} = \bar{H}_2 \quad (9)$$

$$\bar{H}_1(\bar{X}, \bar{t}) = d_1 + a_1 \sin \left\{ \frac{2\pi}{\lambda} (\bar{X} - c\bar{t}) \right\} \quad (10)$$

$$\bar{H}_2(\bar{X}, \bar{t}) = -d_2 - a_2 \sin \left\{ \frac{2\pi}{\lambda} (\bar{X} - c\bar{t}) + \phi \right\} \quad (11)$$

In Eqs. (1) to (11),  $\rho$  is the fluid density,  $\bar{P}$  the pressure,  $T$  the fluid temperature,  $k$  the thermal conductivity,  $U$  the longitudinal velocity component,  $V$  the transverse velocity component,  $a_i$  ( $i = 1, 2$ ),

2) the wave amplitudes at upper and lower walls, respectively,  $\lambda$  the wavelength,  $c$  the wave speed,  $\bar{t}$  the time, and  $\phi$  is the phase difference varying in the range  $0 \leq \phi \leq \pi$  ( $\phi = 0$  leads us to a symmetric channel with waves out of phase and when  $\phi = \pi$ , the waves are in phase). Moreover,  $a_i, d_i$  ( $i = 1, 2$ ) and  $\phi$  satisfy the condition  $a_1^2 + a_2^2 + 2a_1a_2\cos\phi \leq (d_1 + d_2)^2$ .

The extra stress tensor  $\bar{\mathbf{S}}$  for Walter's B fluid (see Ref. 2) is given by

$$\bar{\mathbf{S}} = 2\eta_0\mathbf{e} - 2k_0\frac{\delta\mathbf{e}}{\delta\bar{t}} \quad (12)$$

$$\frac{\delta\mathbf{e}}{\delta\bar{t}} = \frac{\partial\mathbf{e}}{\partial t} + \mathbf{V}\cdot\nabla\mathbf{e} - \mathbf{e}\nabla\mathbf{V} - \nabla\mathbf{V}^T\mathbf{e} \quad (13)$$

where  $\mathbf{e}$  is the rate of strain tensor,  $\partial\mathbf{e}/\delta\bar{t}$  the convected differentiation of the rate of strain tensor in relation to the material in motion,  $\eta_0$  the limiting viscosity at small shear rates, and  $k_0$  is the short memory coefficient.

Defining the following transformations

$$\bar{x} = \bar{X} - c\bar{t}, \quad \bar{y} = \bar{Y}, \quad \bar{u} = \bar{U} - c, \quad \bar{v} = \bar{V}, \quad \bar{p}(\bar{x}, \bar{y}) = \bar{P}(\bar{X}, \bar{Y}, \bar{t}) \quad (14)$$

and considering the non-dimensional relations

$$x = \frac{\bar{x}}{\lambda}, \quad y = \frac{\bar{y}}{d_1}, \quad u = \frac{\bar{u}}{c}, \quad v = \frac{\bar{v}}{c}, \quad p = \frac{d_1^2}{\eta_0\lambda c}\bar{p}, \quad h_1 = \frac{\bar{H}_1}{d_1}, \quad h_2 = \frac{\bar{H}_2}{d_1}, \quad \mathbf{S} = \frac{d_1}{\eta_0 c}\bar{\mathbf{S}}, \quad \delta = \frac{d_1}{\lambda}$$

$$\text{Re} = \frac{\rho c d_1}{\eta_0}, \quad \kappa = \frac{k_0 c}{\eta_0 d_1}, \quad \eta = \frac{T - T_0}{T_1 - T_0}, \quad \text{Er} = \frac{c^2}{\xi(T_1 - T_0)}, \quad \text{Pr} = \frac{\xi \eta_0}{k} \quad (15)$$

where  $\xi$  is the specific heat at constant volume, and then letting the stream function  $\Psi$  related to the velocity components  $u$  and  $v$  by the relations

$$u = \frac{\partial\Psi}{\partial y}, \quad v = -\delta\frac{\partial\Psi}{\partial x} \quad (16)$$

the continuity equation is satisfied and Eqs. (2)–(11) reduce to

$$\delta\text{Re}\left\{\left(\frac{\partial\Psi}{\partial y}\frac{\partial}{\partial x} - \frac{\partial\Psi}{\partial x}\frac{\partial}{\partial y}\right)\frac{\partial\Psi}{\partial y}\right\} = -\frac{\partial p}{\partial x} + \delta\frac{\partial S_{xx}}{\partial x} + \frac{\partial S_{xy}}{\partial y} \quad (17)$$

$$-\delta^3\text{Re}\left\{\left(\frac{\partial\Psi}{\partial y}\frac{\partial}{\partial x} - \frac{\partial\Psi}{\partial x}\frac{\partial}{\partial y}\right)\frac{\partial\Psi}{\partial x}\right\} = -\frac{\partial p}{\partial y} + \delta^2\frac{\partial S_{xy}}{\partial x} + \delta\frac{\partial S_{yy}}{\partial y} \quad (18)$$

$$\delta\text{Re}\left\{\left(\frac{\partial\Psi}{\partial y}\frac{\partial}{\partial x} - \frac{\partial\Psi}{\partial x}\frac{\partial}{\partial y}\right)\nabla^2\Psi\right\} = \left(\frac{\partial^2}{\partial y^2} - \delta^2\frac{\partial^2}{\partial x^2}\right)S_{xy} + \delta\frac{\partial^2}{\partial x\partial y}(S_{xx} - S_{yy}) \quad (19)$$

$$\delta\text{Re}\left(\frac{\partial\Psi}{\partial y}\frac{\partial\eta}{\partial x} - \frac{\partial\Psi}{\partial x}\frac{\partial\eta}{\partial y}\right) = \frac{1}{\text{Pr}}\left(\delta^2\frac{\partial^2\eta}{\partial x^2} + \frac{\partial^2\eta}{\partial y^2}\right) + \text{Er}\left\{\delta\Psi_{xy}S_{xx} + (\Psi_{yy} - \delta^2\Psi_{xx})S_{xy} - \delta\Psi_{xy}S_{yy}\right\} \quad (20)$$

where  $\nabla^2 = \delta^2\frac{\partial^2}{\partial x^2} + \frac{\partial^2}{\partial y^2}$ .

$$S_{xx} = 4\delta\Psi_{xy} - \kappa(4\delta^2\Psi_y\Psi_{xxy} - 4\delta^2\Psi_x\Psi_{xyy} - 8\delta\Psi_{xy}^2 + 4\delta^2\Psi_{xx}\Psi_{yy} - 4\delta^4\Psi_{xx}^2) \quad (21)$$

$$S_{xy} = 2(\Psi_{yy} - \delta^2\Psi_{xx}) - \kappa(2\delta\Psi_y\Psi_{xyy} - 2\delta^3\Psi_y\Psi_{xxx} - 2\delta\Psi_x\Psi_{yyy} + 2\delta^3\Psi_x\Psi_{xyy} - 6\delta\Psi_{xy}\Psi_{yy})$$

$$+2\delta\Psi_{yy}\Psi_{xy} + 2\delta^3\Psi_{xy}\Psi_{xx} - 6\delta^3\Psi_{xx}\Psi_{xy}) \quad (22)$$

$$S_{yy} = -4\delta\Psi_{xy} - \kappa(-4\delta^2\Psi_y\Psi_{xxy} + 4\delta^2\Psi_x\Psi_{xyy} - 4\Psi_{yy}^2 + 4\delta^2\Psi_{xx}\Psi_{yy} - 8\delta^2\Psi_{xy}^2) \quad (23)$$

with boundary conditions

$$\Psi = \frac{F}{2}, \quad \frac{\partial\Psi}{\partial y} = -1, \quad \eta = 0, \quad \text{at} \quad y = h_1(x) \quad (24)$$

$$\Psi = -\frac{F}{2}, \quad \frac{\partial\Psi}{\partial y} = -1, \quad \eta = 1, \quad \text{at} \quad y = h_2(x) \quad (25)$$

$$h_1(x) = 1 + a\sin(2\pi x), \quad \text{and} \quad h_2(x) = -d - b\sin(2\pi x + \phi) \quad (26)$$

Here  $Re$  is the Reynolds number,  $\kappa$  the viscoelastic parameter,  $Er$  the Eckert number,  $Pr$  the Prandtl number, and  $a = (a_1/d_1)$ ,  $b = (a_2/d_1)$ ,  $d = (d_2/d_1)$  satisfy the condition

$$a^2 + b^2 + 2ab\cos\phi \leq (1+d)^2 \quad (27)$$

and  $F$  is the dimensionless average flux in the wave frame defined by

$$F = \int_{h_2(x)}^{h_1(x)} \frac{\partial\Psi}{\partial y} dy = \Psi(h_1(x)) - \Psi(h_2(x)) \quad (28)$$

which is related to  $\theta$  the dimensionless average flux in the laboratory frame, by the relation

$$\theta = F + 1 + d \quad (29)$$

The dimensionless pressure rise per wavelength  $\Delta p_\lambda$  and heat transfer coefficient  $Z_{h_1}$  and  $Z_{h_2}$  at upper and lower walls are calculated by the relation

$$\Delta p_\lambda = \int_0^1 \frac{dp}{dx} \Big|_{y=0} dx, \quad Z_{h_1} = \frac{\partial h_1}{\partial x} \frac{\partial \eta}{\partial y}, \quad Z_{h_2} = \frac{\partial h_2}{\partial x} \frac{\partial \eta}{\partial y} \quad (30)$$

### 3. Solution of the Problem

Equations (17) to (23) with boundary conditions (24) and (25) are solved analytically using the regular perturbation method. For perturbation solutions we expand the flow quantities in terms of small wave number  $\delta$  ( $\delta \ll 1$ ) as

$$\Psi = \sum_{i=0}^{\infty} \delta^i \Psi_i, \quad \mathbf{S} = \sum_{i=0}^{\infty} \delta^i \mathbf{S}_i, \quad \eta = \sum_{i=0}^{\infty} \delta^i \eta_i, \quad Z = \sum_{i=0}^{\infty} \delta^i Z_i \quad (31)$$

After substituting Eq. (31) into Eqs. (17)–(23) with boundary conditions (24) and (25) and comparing the coefficients of powers of  $\delta$  we obtain the system of equations as follows.

#### 3.1 Zeroth-order system

The zeroth-order system is

$$\frac{\partial^2 S_{0xy}}{\partial y^2} = 0 \quad (32)$$

$$\frac{1}{Pr} \frac{\partial^2 \eta_0}{\partial y^2} + 2Er\Psi_{0yy}^2 = 0 \quad (33)$$

$$S_{0xx} = 0, S_{0xy} = 2\Psi_{0yy}, S_{0yy} = 4\kappa\Psi_{0yy}^2 \quad (34)$$

where the boundary conditions are

$$\Psi_0 = \frac{F_0}{2}, \quad \frac{\partial\Psi_0}{\partial y} = -1, \quad \eta_0 = 0, \quad \text{at } y = h_1(x) \quad (35)$$

$$\Psi_0 = -\frac{F_0}{2}, \quad \frac{\partial\Psi_0}{\partial y} = -1, \quad \eta_0 = 1, \quad \text{at } y = h_2(x) \quad (36)$$

Substituting Eq. (34) into Eqs. (32) and (33) and then solving the resulting system with boundary conditions (35) and (36), we obtain the solutions up to  $O(S^0)$  as

$$S_{0xy} = 4A_3 + 12A_4y \quad (37)$$

$$\Psi_0 = A_1 + A_2y + A_3y^2 + A_4y^3 \quad (38)$$

$$\eta_0 = S_1 + S_2y + S_3y^2 + S_4y^3 + S_5y^4 \quad (39)$$

$$Z_{0h_1} = a \cos x (S_2 + 2S_3y + 3S_4y^2 + 4S_5y^3) \quad (40)$$

$$Z_{0h_2} = -b \cos(x + \phi) (S_2 + 2S_3y + 3S_4y^2 + 4S_5y^3) \quad (41)$$

### 3.2 First-order system

The first-order system is

$$\frac{\partial^2 S_{1xy}}{\partial y^2} + \frac{\partial^2 S_{0xx}}{\partial x \partial y} = \frac{\partial^2 S_{0yy}}{\partial x \partial y} + \text{Re}(\Psi_{0y} \Psi_{0xyy} - \Psi_{0x} \Psi_{0yyy}) \quad (42)$$

$$\frac{1}{\text{Pr}} \frac{\partial^2 \eta_1}{\partial y^2} + \text{Er} \Phi_1 = \text{Re}(\Psi_{0y} \eta_{0x} - \Psi_{0x} \eta_{0y}) \quad (43)$$

$$S_{1xx} = 4\Psi_{0xy} + 8\kappa\Psi_{0xy}^2 \quad (44)$$

$$S_{1xy} = 2\Psi_{1yy} - 2\kappa\Psi_{0y} \Psi_{0xyy} + 2\kappa\Psi_{0x} \Psi_{0yyy} + 4\kappa\Psi_{0xy} \Psi_{0yy} \quad (45)$$

$$S_{1yy} = 8\kappa\Psi_{0yy} \Psi_{1yy} - 4\Psi_{0xy} \quad (46)$$

$$\Phi_1 = 4\Psi_{0yy} \Psi_{1yy} - 2\kappa\Psi_{0y} \Psi_{0yy} \Psi_{0xyy} + 2\kappa\Psi_{0x} \Psi_{0yy} \Psi_{0yyy} + 6\kappa\Psi_{0xy} \Psi_{0yy}^2 - 6\kappa\Psi_{0xy} \Psi_{0xy} \quad (47)$$

where the boundary conditions are

$$\Psi_1 = \frac{F_1}{2}, \quad \frac{\partial\Psi_1}{\partial y} = 0, \quad \eta_1 = 0, \quad \text{at } y = h_1(x) \quad (48)$$

$$\Psi_1 = -\frac{F_1}{2}, \quad \frac{\partial\Psi_1}{\partial y} = 0, \quad \eta_1 = 0, \quad \text{at } y = h_2(x) \quad (49)$$

Using the zeroth-order solutions Eqs. (37)–(41) into first-order system Eqs. (42)–(47) and then solving the resulting system we obtain

$$S_{1xy} = L_{37} + L_{38}y + L_{39}y^2 + L_{40}y^3 + L_{41}y^4 + L_{42}y^5 \quad (50)$$

$$\Psi_1 = B_1 + B_2y + B_3y^2 + B_4y^3 + B_5y^4 + B_6y^5 + B_7y^6 + B_8y^7 \quad (51)$$

$$\eta_1 = S_6 + S_7y + S_8y^2 + S_9y^3 + S_{10}y^4 + S_{11}y^5 + S_{12}y^6 + S_{13}y^7 + S_{14}y^8 \quad (52)$$

$$Z_{1h_1} = a \cos x (S_7 + 2S_8y + 3S_9y^2 + 4S_{10}y^3 + 5S_{11}y^4 + 6S_{12}y^5 + 7S_{13}y^6 + 8S_{14}y^7) \quad (53)$$

$$Z_{1/h_2} = -b \cos(x + \phi)(S_7 + 2S_8y + 3S_9y^2 + 4S_{10}y^3 + 5S_{11}y^4 + 6S_{12}y^5 + 7S_{13}y^6 + 8S_{14}y^7) \quad (54)$$

All the coefficients appearing in the above expressions of the solutions are calculated by the usual lengthy algebra that is involved in the regular perturbation method.

#### 4. Discussion

The effects of viscoelastic parameter  $\kappa$ , Prandtl number  $Pr$ , Eckert number  $Er$ , and phase difference  $\phi$  appearing in the solutions of stream function  $\Psi$ , temperature distribution  $\eta$ , and heat transfer coefficient  $Z$  are presented graphically in this section. The comparison of the present series solution for pressure rise per wave length  $\Delta p_\lambda$  for different flow rate  $\theta$  is presented in Table 1. These results are found in good agreement with those reported by Mishra and Rao [15].

Figures 1 and 2 display the changes in temperature distribution  $\eta$  against  $y$  due to variation of parameters  $Er$ ,  $Pr$ , and  $\theta$ . As expected, the temperature profiles are almost parabolic concaved downward. These temperature profiles are greater near the upper wall which parabolically decreases moving toward the lower wall. It is worth mentioning that in Fig. 1(i) with the absence of viscous dissipation ( $Er = 0$ ) the temperature profile is linear. Further, it is noticed in this figure and Fig. 1(ii) that the temperature profiles increase with an increasing  $Pr$  and  $Er$ . Figure 2(i) shows that temperature profiles decrease with an increasing  $\theta (< 1)$ , whereas in Fig. 2(ii) the temperature profiles increase with an increasing  $\theta (> 1)$ .

Finally, Figs. 3 to 6 present the coefficients of heat transfer  $Z_{h_1}$  and  $Z_{h_2}$  for different values of  $Er$ ,  $Pr$ ,  $\kappa$ , and  $\phi$  at the upper and lower walls, respectively. An oscillatory behavior is observed in all figures which is due to the propagation of peristaltic waves along the walls of the channel. Further, it is noticed that the absolute value of the heat transfer coefficient increases with an increasing  $Er$ ,  $Pr$ , and  $\kappa$ . It is also noted in Fig. 6 that the absolute value of the heat transfer coefficient increases at the upper wall but decreases at the lower wall of the channel with an increasing  $\phi$ .

Table 1. Comparison of Pressure Rise Per Wavelength  $\Delta p_\lambda$  for Different Values of Flow Rate  $\theta$  When  $a = 0.7$ ,  $b = 1.2$ ,  $d = 2$ ,  $\kappa = 0$ ,  $\delta = 0$ ,  $Re = 0$

$\theta$	$\Delta p_\lambda(\phi = 0)$		$\Delta p_\lambda(\phi = \pi)$	
	Mishra and Rao [15]	Present results	Mishra and Rao [15]	Present results
-1.0	4.8126	4.812560	0.5431	0.543106
-0.5	3.8514	3.851390	0.3014	0.301358
0.0	2.8902	2.890210	0.0596	0.059609
0.5	1.9290	1.929030	-0.1821	-0.182139
1.0	0.9679	0.967850	-0.4239	-0.423888
1.5	0.0067	0.006672	-0.6656	-0.665637
2.0	-0.9545	-0.954507	-0.9074	-0.907385
2.5	-1.9157	-1.915690	-1.1491	-1.149130
3.0	-2.8769	-2.876860	-1.3909	-1.390880

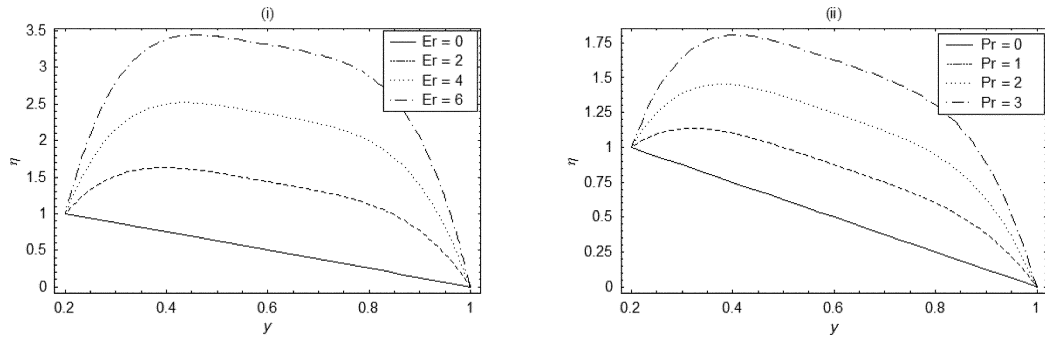


Fig. 1. Temperature profile  $\eta$  for fixed  $a = 0.5, b = 1.2, d = 1, \phi = \pi/2, \theta = 1, \kappa = 0.1, \delta = 0.01, Re = 5, x = 0.5$  (i)  $Pr = 5$  (ii)  $Er = 4$ .

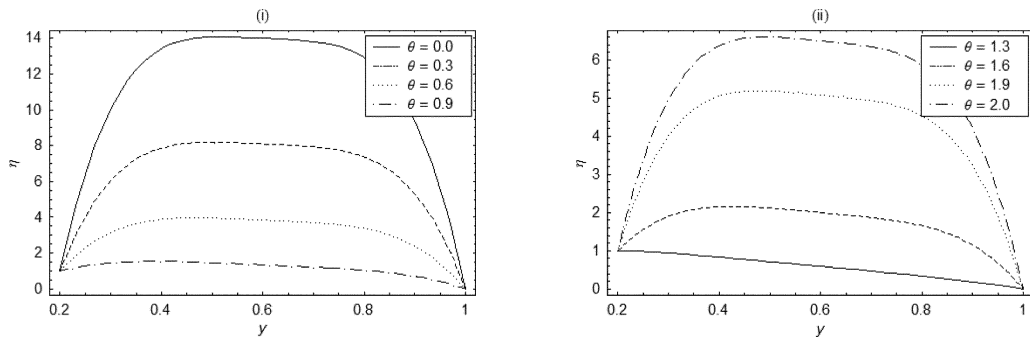


Fig. 2. Temperature profile  $\eta$  for fixed  $a = 0.5, b = 1.2, d = 1, \phi = \pi/2, \kappa = 0.1, \delta = 0.01, Re = 5, x = 0.5, Pr = 1, Er = 4$  (i)  $\theta < 1$  (ii)  $\theta > 1$ .

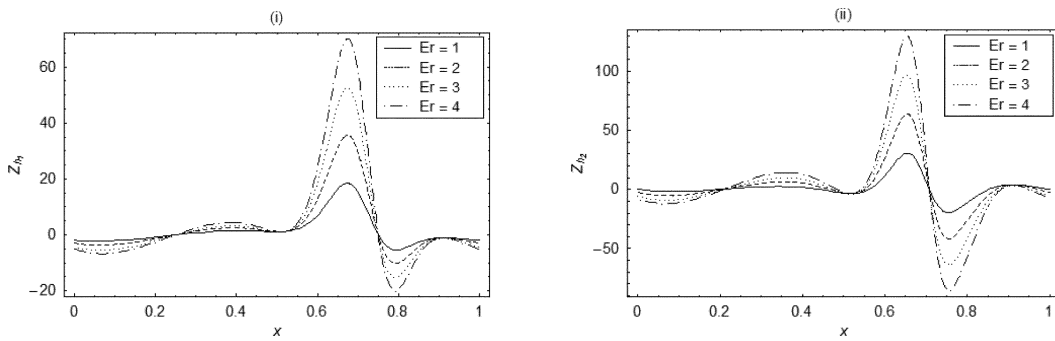


Fig. 3. Heat transfer coefficient (i)  $Z_{h_1}$  at upper wall (ii)  $Z_{h_2}$  at lower wall for fixed  $a = 0.4, b = 1.2, d = 1.5, \phi = \pi/12, \theta = 1, \kappa = 0.1, \delta = 0.01, Re = 1, Pr = 1$ .

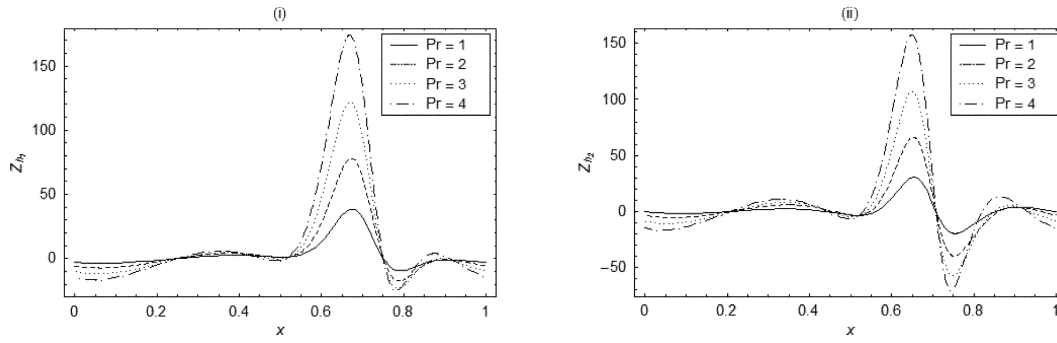


Fig. 4. Heat transfer coefficient (i)  $Z_{h_1}$  at upper wall (ii)  $Z_{h_2}$  at lower wall for fixed  $a = 0.4, b = 1.2, d = 1.5, \phi = \pi/12, \theta = 0.5, \kappa = 1, \delta = 0.01, Re = 1, Er = 2$ .

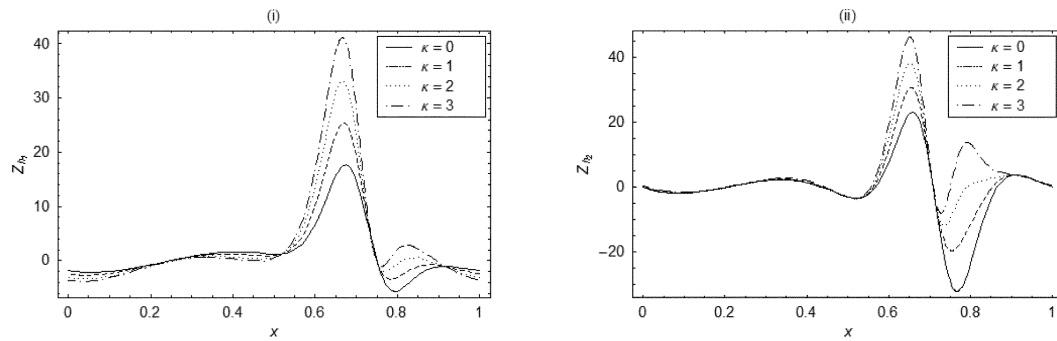


Fig. 5. Heat transfer coefficient (i)  $Z_{h_1}$  at upper wall (ii)  $Z_{h_2}$  at lower wall for fixed  $a = 0.4, b = 1.2, d = 1.5, \phi = \pi/12, \theta = 0.5, \delta = 0.01, Re = 1, Er = 2, Pr = 1$ .

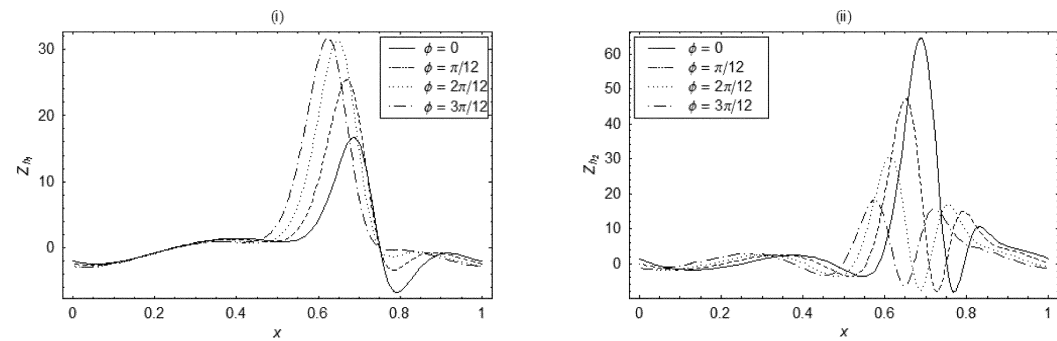


Fig. 6. Heat transfer coefficient (i)  $Z_{h_1}$  at upper wall (ii)  $Z_{h_2}$  at lower wall for fixed  $a = 0.4, b = 1.2, d = 1.5, \theta = 0.5, \kappa = 1, \delta = 0.03, Re = 1, Er = 1, Pr = 1$ .

## 5. Conclusion

In this study the problem of heat transfer on the peristaltic flow of a Walter's B fluid in a two-dimensional asymmetric channel is considered. The resulting equations containing viscoelastic parameter  $\kappa$ , Eckert number  $Er$ , Prandtl number  $Pr$ , and phase difference  $\phi$  are solved analytically by taking the wave number as the small parameter. It is concluded that the temperature profiles are parabolic and significant variations lie in the center of the channel due to the viscous dissipation. In the absence of viscous dissipation the temperature profile becomes linear. Temperature of the fluid increases with an increasing Eckert and Prandtl number. The behavior of the heat transfer coefficient is oscillatory due to the propagation of peristaltic waves. Further the absolute value of the heat transfer coefficient increases with an increasing viscoelastic parameter.

## Acknowledgments

The authors would like to acknowledge the Ministry of Higher Education (MOHE) and Research Management Centre—UTM for the financial support through vote numbers 03J54, 78528, and 4F109 for this research.

## Literature Cited

1. Shapiro AH, Jaffrin MY, Weinberg SL. Peristaltic pumping with long wavelength at low Reynolds number. *J Fluid Mech* 1969;37:799–825.
2. Beard DW, Walters K. Elastico-viscous boundary-layer flows. Part I. Two-dimensional flow near a stagnation point. *Proc Camb Phil Soc* 1964;60:667–674.
3. Baris S. Steady flow of a Walter's B viscoelastic fluid between a porous elliptic plate and a ground. *Turkish J Eng Env Sci* 2002;26:403–418.
4. Joneidi AA, Domairry G, Babaelahi M. Homotopy analysis method to Walter's B fluid in a vertical channel with porous wall. *Meccanica* 2010;45:857–868.
5. Nandeppanavar MM, Abel MS, Tawade J. Heat transfer in a Walter's B fluid over an impermeable stretching sheet with non-uniform heat source/sink and elastic deformation. *Commun Nonlinear Sci Numer Simulat* 2010;15:1791–1802.
6. Ali N, Sajid M, Javed T, Abbas Z. Heat transfer analysis of peristaltic flow in a curved channel. *Int J Heat Mass Transf* 2010;53:3319–3325.
7. Hayat T, Mehmood OU. Slip effects on MHD flow of third order fluid in a planar channel. *Commun Nonlinear Sci Numer Simulat* 2011;16:1363–1377.
8. Muthuraj R, Srinivas S. A note on heat transfer to MHD oscillatory flow in an asymmetric wavy channel. *Int Commun Heat Mass Transf* 2010;37:1255–1260.
9. Srinivas S, Gayathri R, Kothandapani M. The influence of slip conditions, wall properties and heat transfer on MHD peristaltic transport. *Comp Phys Commun* 2009;180:2115–2122.
10. Hayat T, Hina S, Hendi AA. Heat and mass transfer effects on peristaltic flow of an Oldroyd-B fluid in a channel with compliant walls. *Heat Trans Asian Res* 2012;41:63–83.
11. Srinivas S, Kothandapani M. Peristaltic transport in an asymmetric channel with heat transfer—A note. *Int Commun Heat Mass Transf* 2008;35:514–522.
12. Vajravelu K, Sreenadh S, Lakshminarayana P. The influence of heat transfer on peristaltic transport of a Jeffrey fluid in a vertical porous stratum. *Commun Nonlinear Sci Numer Simulat* 2011;16:3107–3125.
13. Nadeem S, Akbar NS. Peristaltic flow of Walter's B fluid in a uniform inclined tube. *J Biorheol* 2010;24:22–28.

14. Nadeem S, Akbar NS, Hayat T, Henci AA. Peristaltic flow of Walter's B fluid in endoscope. *Appl Math Mech Engl Ed* 2011;32:689–700.
15. Mishra M, Rao AR. Peristaltic flow of Newtonian fluid in an asymmetric channel. *Zeit Angew Math Phys* 2003;54:532–550.

